

AFAPL-TR-79-2124

LEVEL

2

ADA 083434

EVALUATION OF LOW MELTING HALIDE SYSTEMS FOR BATTERY APPLICATIONS

Department of Chemistry
The University of Tennessee
Knoxville, Tennessee 37916

APR 23 1980
C

November 1979

TECHNICAL REPORT AFAPL-TR-79-2124

Interim Report for the Period 1 September 1978 through 31 August 1979

Approved for public release; distribution unlimited.

DDC FILE COPY

AIR FORCE AERO PROPULSION LABORATORY
AIR FORCE WRIGHT AERONAUTICAL LABORATORIES
AIR FORCE SYSTEMS COMMAND
WRIGHT-PATTERSON AIR FORCE BASE, OHIO 45433

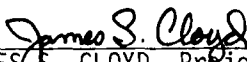
84 4 21 050


NOTICE

When Government drawings, specifications, or other data are used for any purpose other than in connection with a definitely related Government procurement operation, the United States Government thereby incurs no responsibility nor any obligation whatsoever; and the fact that the government may have formulated, furnished, or in any way supplied the said drawings, specifications, or other data, is not to be regarded by implication or otherwise as in any manner licensing the holder or any other person or corporation, or conveying any rights or permission to manufacture, use, or sell any patented invention that may in any way be related thereto.

This report has been reviewed by the Information Office (OI) and is releasable to the National Technical Information Service (NTIS). At NTIS, it will be available to the general public, including foreign nations.

This technical report has been reviewed and is approved for publication.


JAMES S. CLOYD, Project Engineer
Batteries & Fuel Cells


DONALD P. MORTEL, Actg. Chief
Energy Conversion Branch

FOR THE COMMANDER


JAMES D. REAMS, Chief
Aerospace Power Division
Aero Propulsion Laboratory

"If your address has changed, if you wish to be removed from our mailing list, or if the addressee is no longer employed by your organization please notify AFWAL/POOC-1, W-PAFB, OH 45433 to help us maintain a current mailing list"

Copies of this report should not be returned unless return is required by security considerations, contractual obligations, or notice on a specific document.

REPORT DOCUMENTATION PAGE		READ INSTRUCTIONS BEFORE COMPLETING FORM
1. REPORT NUMBER AFAPL-TR-79-2124 ✓	2. GOVT ACCESSION NO.	3. RECIPIENT'S CATALOG NUMBER
4. TITLE (and Subtitle) Evaluation of Low Melting Halide Systems for Battery Applications		5. TYPE OF REPORT & PERIOD COVERED Interim / 1 Sep 78 AFAPL 31 Aug 79
7. AUTHOR(s) Dr. Gleb Mamantov		6. PERFORMING ORG. REPORT NUMBER
9. PERFORMING ORGANIZATION NAME AND ADDRESS University of Tennessee Department of Chemistry Knoxville TN 37916		8. CONTRACT OR GRANT NUMBER(s) AF Contract No. F33615-78-C-20670-2075
11. CONTROLLING OFFICE NAME AND ADDRESS Air Force Aero Propulsion Laboratory Wright-Patterson AFB Ohio 45433		10. PROGRAM ELEMENT, PROJECT, TASK AREA & WORK UNIT NUMBERS 31452289
14. MONITORING AGENCY NAME & ADDRESS (if different from Controlling Office)		12. REPORT DATE November 1979
		13. NUMBER OF PAGES 39
		15. SECURITY CLASS. (of this report) UNCLASSIFIED
		15a. DECLASSIFICATION DOWNGRADING SCHEDULE
16. DISTRIBUTION STATEMENT (of this Report) Approved for public release; distribution unlimited		
17. DISTRIBUTION STATEMENT (of the abstract entered in Block 20, if different from Report)		
18. SUPPLEMENTARY NOTES		
19. KEY WORDS (Continue on reverse side if necessary and identify by block number) electrolytes, molten salt, low melting point, conductivity		
20. ABSTRACT (Continue on reverse side if necessary and identify by block number) This three year program involves evaluation of selected low temperature molten salt solvent systems containing inorganic and/or organic chlorides and bromides for battery applications. The research involves determination of the liquidus temperatures, the specific electrical conductivity, and the electrochemical span of selected halide systems. Characterization of the solvent species by Raman spectroscopy, vapor pressure measurements, and the electrochemical study of a few cathode and anode systems will be undertaken for the (Cont)		

most promising solvent systems.

The research during the first year of this project involved the determination of liquidus temperatures for a number of binary and ternary chloro- and bromoaluminate systems, and the specific electrical conductivity studies of the AlCl_3 -LiCl-NaCl system.

FOREWORD

This report describes the work performed during the first year of a three-year program dealing with the experimental evaluation of some low melting halide systems for battery applications. This work was performed at the Department of Chemistry, The University of Tennessee, Knoxville, under Contract No. F33615 78-C-2075 with the U. S. Air Force Aero Propulsion Laboratory, Wright-Patterson Air Force Base, Ohio. The principal investigator is Professor Gleb Mamantov. The Air Force Project officer is Mr. J. S. Cloyd, AFAPL/POE-1, Wright-Patterson Air Force Base, Ohio.

The personnel working on the project consisted of Dr. Cedomir Petrovic, postdoctoral research associate, Jeff Ledford, Walter Li, Jeff Nelson, and Robert Walton, undergraduate research assistants.

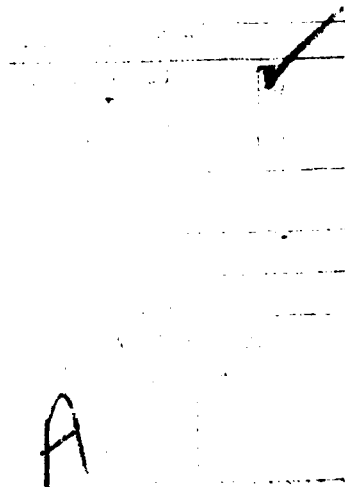


TABLE OF CONTENTS

SECTION	DESCRIPTION	PAGE
1	INTRODUCTION AND SCIENTIFIC BACKGROUND	1
2	LIQUIDUS RANGE STUDIES	1
	2.1 EXPERIMENTAL	1
	2.2 DETERMINATION OF LIQUIDUS RANGE FROM DSC DATA	2
	2.3 AlCl_3 -LiCl-NaCl SYSTEM	3
	2.4 OTHER TERNARY AlCl_3 -MCl SYSTEMS	5
	2.5 AlCl_3 - BaCl_2 -NaCl SYSTEM	5
	2.6 AlCl_3 - CaCl_2 -NaCl SYSTEM	9
	2.7 AlCl_3 -NaBr SYSTEM	9
	2.8 AlBr_3 - R_4NBr SYSTEM	11
	2.9 AlBr_3 - Bu_4NBr SYSTEM	14
	2.10 AlBr_3 - Me_4NBr SYSTEM	14
3.	ELECTRICAL CONDUCTIVITY STUDIES	15
	3.1 EXPERIMENTAL	15
	3.2 AlCl_3 -LiCl-NaCl SYSTEM	15
	3.3 MEASUREMENTS IN THE SOLID PHASE	17
	REFERENCES	36

LIST OF ILLUSTRATIONS

FIGURE	DESCRIPTION	PAGE
1	DSC RECORDINGS OF 61.0-39.0 MOLE % AlCl_3 -NaCl AT SENSITIVITY OF 2, 10, AND 20 mcal/sec FULL SCALE	4
2	PHASE DIAGRAM DATA FOR AlCl_3 -LiCl-NaCl SYSTEM	7
3	PHASE DIAGRAM DATA FOR AlCl_3 -NaBr, AlCl_3 -NaCl AND AlBr_3 -NaBr SYSTEMS	13
4	ELECTRICAL CONDUCTIVITY CELL	16
5	SPECIFIC CONDUCTIVITY OF AlCl_3 -LiCl-NaCl SYSTEM (LiCl-NaCl MOLE RATIO 1:1)	31
6	SPECIFIC CONDUCTIVITY OF AlCl_3 -LiCl-NaCl SYSTEM (LiCl-NaCl MOLE RATIO 3:1)	32
7	RECIPROCAL RESISTANCE AND CAPACITANCE OF 54.0-23.0-23.0 MOLE % AlCl_3 -LiCl-NaCl AND OF 66.0-34.0 MOLE % AlCl_3 -NaCl	35

LIST OF TABLES

TABLE	DESCRIPTION	PAGE
1	PHASE DIAGRAM DATA FOR AlCl_3 -LiCl-NaCl SYSTEM	6
2	PHASE DIAGRAM DATA FOR OTHER TERNARY ALKALI CHLOROALUMI-NATE SYSTEMS	8
3	PHASE DIAGRAM DATA FOR AlCl_3 - BaCl_2 -NaCl SYSTEM	10
4	PHASE DIAGRAM DATA FOR AlCl_3 - CaCl_2 -NaCl SYSTEM	10
5	PHASE DIAGRAM DATA FOR AlCl_3 -NaBr SYSTEM	12
6	SPECIFIC CONDUCTIVITY OF 52.0-24.0-24.0 MOLE % AlCl_3 -LiCl-NaCl	18
7	SPECIFIC CONDUCTIVITY OF 54.0-23.0-23.0 MOLE % AlCl_3 -LiCl-NaCl	19
8	SPECIFIC CONDUCTIVITY OF 56.0-22.0-22.0 MOLE % AlCl_3 -LiCl-NaCl	20
9	SPECIFIC CONDUCTIVITY OF 58.0-21.0-21.0 MOLE % AlCl_3 -LiCl-NaCl	21
10	SPECIFIC CONDUCTIVITY OF 60.0-20.0-20.0 MOLE % AlCl_3 -LiCl-NaCl	22
11	SPECIFIC CONDUCTIVITY OF 62.0-19.0-19.0 MOLE % AlCl_3 -LiCl-NaCl	23
12	SPECIFIC CONDUCTIVITY OF 64.0-18.0-18.0 MOLE % AlCl_3 -LiCl-NaCl	24
13	SPECIFIC CONDUCTIVITY OF 68.0-16.0-16.0 MOLE % AlCl_3 -LiCl-NaCl	25
14	SPECIFIC CONDUCTIVITY OF 53.4-35.0-11.6 MOLE % AlCl_3 -LiCl-NaCl	26
15	SPECIFIC CONDUCTIVITY OF 56.0-33.0-11.0 MOLE % AlCl_3 -LiCl-NaCl	27
16	SPECIFIC CONDUCTIVITY OF 58.0-31.5-10.5 MOLE % AlCl_3 -LiCl-NaCl	28
17	SPECIFIC CONDUCTIVITY OF 60.0-30.0-10.0 MOLE % AlCl_3 -LiCl-NaCl	29

LIST OF TABLES

Page 2

TABLE	DESCRIPTION	PAGE
18	SPECIFIC CONDUCTIVITY OF 68.0-24.0-8.0 MOLE % AlCl_3 - LiCl-NaCl	30
19	TEMPERATURE DEPENDENCE OF SPECIFIC CONDUCTIVITY OF AlCl_3 - LiCl-NaCl SYSTEM	33

1. INTRODUCTION AND SCIENTIFIC BACKGROUND

Molten alkali chloroaluminates are of considerable recent interest as solvents in several primary and secondary batteries presently under development (1-3). They have low liquidus temperatures, a relatively large electrochemical span and good specific electrical conductivity. For example, the liquidus temperature of the AlCl_3 - NaCl binary molten salt system varies as a function of composition between 115 and 190°C; the potential span between the aluminum deposition and the chlorine evolution is 2.1 V, and the specific conductivity is in the 0.1-0.7 $\text{ohm}^{-1}\text{cm}^{-1}$ range (4). The acid-base properties of an aluminum chloride-alkali chloride system are a function of its composition (5). Thus, the chloride ion concentration in these melts which describes the Lewis acidity can be readily varied over several decades (5).

Even lower liquidus temperatures are possible in chloroaluminate melts in which an organic halide is substituted for an alkali halide. For example, some compositions of AlCl_3 -1-ethylpyridinium chloride and AlCl_3 -1-ethylpyridinium bromide are liquid at room temperatures (6-8). The former melt system is being studied at the F. J. Seiler Research Laboratory for possible battery applications (9).

Other low-temperature melt systems may be useful for battery applications. Recent compilations list a number of binary and/or ternary systems in which AlCl_3 , AlBr_3 , GaCl_3 , GaBr_3 , SbCl_3 and FeCl_3 , among others, appear as one component (10,11). These compilations do not attempt a critical evaluation of existing data and much of the information listed in them is conflicting. The more critical recent volume by Janz et. al. (4) includes only a few chloroaluminate molten salt systems. Low melting salt systems which do not contain AlCl_3 , such as AlBr_3 , GaCl_3 and FeCl_3 containing melts, have received little attention to date as possible solvents for battery uses.

The purpose of this three year project is to critically evaluate a wide range of binary and ternary low temperature molten salt systems for battery applications. These systems include chlorides and bromides of aluminum, antimony, gallium and iron as one component, and various alkali, alkaline earth and quaternary ammonium halides as the other(s). Measurements of the liquidus range and the specific electrical conductivity will be performed on a number of the above systems. Vapor pressure, background voltammograms and Raman spectra will be studied for a few selected systems. Electrochemistry of selected cathode and anode materials will also be examined. This is a report of the first year of the work. Two types of studies were pursued during this period: the measurements of the liquidus range, using differential scanning calorimetry, and of the specific electrical conductivity by the conventional AC technique.

2. LIQUIDUS RANGE STUDIES

2.1. Experimental

Samples of the melts studied in the present work were prepared by the standard procedures employed in our Laboratory. Anhydrous aluminum chloride

(Fluka, puris, distilled) was digested overnight at 210°C with high purity aluminum (Alfa-Ventron, m6N) in evacuated, sealed glass vessels and subsequently redistilled in the same vessels. Anhydrous aluminum bromide (Fluka, purum, distilled) was digested at 140°C and redistilled in the same manner. Alkali chlorides and bromides (Fisher and Baker), calcium chloride (Mallinckrodt, anhydrous), and barium chloride (Vaughn, anhydrous) were dried in vacuum at 400°C for five days. Tetrabutyl ammonium bromide (Eastman) was dried in vacuum at 90°C for seven days; tetramethyl ammonium bromide (Eastman) was dried at 160°C for the same length of time.

Samples of the melts, 6-10 g for each composition, were prepared using an analytical balance in a dry box (Vacuum Atmospheres), with the moisture and oxygen levels of <2 ppm. In view of the very small size of samples used in the DSC experiments (1.5 to 2.0 mg), special care was taken to insure that the DSC samples were representative of the average composition of the solid samples. The samples were prepared in specially designed melt tubes with thin walled capillary sidearms. By quenching these sample tubes in an ice-water bath, the melt in the sidearms was rapidly frozen. Samples for the DSC measurements were taken from these sidearms and sealed in aluminum sample pans (Perkin Elmer Co.) in the dry box, and were kept under dry nitrogen atmosphere until and during the DSC experiments.

A commercial differential scanning calorimeter, Perkin Elmer DSC-1B, was used to determine the phase transition temperatures. The data were recorded on a Moseley Autograph 2D-2A X-Y recorder with 5mV full scale sensitivity. A low pass RC filter was used to reduce the noise. An Analog Devices amplifier, Model AD 521, was occasionally used to increase the sensitivity of the instrument. The samples were scanned at 5°C/min. At this slow speed no appreciable instrumental distortion of the DSC curves was noticed. The calorimeter was calibrated at the same scanning speed with sealed high purity indium and tin standards with the melting temperatures of 156.2 and 231.9°C, respectively. Only the melting curves were used for collecting the data. Due to severe supercooling, of the order of 20-50°C, the cooling curves were of little value for our work.

2.2. Determination of Liquidus Range from DSC Data

In our last two quarterly reports, the first deviation of the melting peak from the baseline in the DSC recordings was interpreted as the solidus temperature. In the present report, however, all DSC data have been reinterpreted. The solidus temperature in Tables 1.1 to 1.5 is the "extrapolated onset" temperature, *i.e.* the intersection of the extrapolated linear section of the ascending melting peak with the extrapolated baseline. Our "extrapolated onset" value for the solidus temperature of the AlCl₃-NaCl samples, 114°C, was in good agreement with the literature value of 115°C (12), obtained by the visual observation technique. Our "first deviation" value of 104°C for the same system, however, was in fair agreement with the more recent literature value of 107.2°C (13), also determined by the visual method. Since there is no agreement in the literature regarding the correct method of extracting the melting temperatures from the DSC data (14-16), the "first deviation", the "extrapolated onset", and the peak maximum temper-

atures having been used, an independent experimental method was sought to resolve this issue.

Our measurements of the electrical conductivity of the solid alkali chloroaluminates (discussed in more detail in Section 3.3) did not yield an unambiguous solidus temperature. Even though the conductivity change during the melting process was nearly four orders of magnitude, the change itself was gradual and difficult to interpret.

The interpretation of the results was assisted by performing DSC experiments at the Oak Ridge National Laboratory, using the Perkin-Elmer DSC-2 instrument, which has a superior sensitivity and signal-to-noise ratio, as well as a flat baseline. These experiments demonstrated that the "first deviation" temperature is a function of the sensitivity limit of the instrument (Figure 1). In our measurements with the DSC-1B instrument the "first deviation" temperature is determined by a combination of the maximum amplifier gain, the instrumental noise level, and the baseline curvature, and, therefore, does not have much physical meaning.

The change in the method of reading of the solidus temperature in this Report also necessitated a change in the reading of the liquidus temperature. If the "extrapolated onset" temperature is the true melting point of a pure compound, and if the slope of the leading edge of its melting peak is determined by the thermal resistance of the sample pan--sample interface and of the sample itself (14), then the sample of that pure compound is completely molten by the time the maximum of the melting peak is reached (16). In that case the liquidus temperature of a multicomponent sample is neither the temperature of the return to the baseline, nor the "extrapolated return" temperature in the DSC recordings, because the multicomponent system is presumably also completely molten by the time the last maximum of the melting curve is reached. Therefore, the maximum of the last peak should be read as the liquidus temperature. The thermal resistance probably plays a role here as well, but it is not clear whether it is necessary to perform the thermal lag correction in this case. The liquidus temperature data in this Report (Tables 1.1 to 1.5) were read as the extrapolated maxima of the last melting peak in the DSC recordings, and are not corrected for the thermal lag.

2.3. $\text{AlCl}_3\text{-LiCl-NaCl}$ System

The $\text{AlCl}_3\text{-LiCl-NaCl}$ molten salt system appears attractive as a solvent for battery use. The addition of LiCl to the $\text{AlCl}_3\text{-NaCl}$ system, the most widely used of the chloroaluminate systems, lowers the liquidus range of the latter without altering drastically most of its other physical and chemical properties. The ionic mobility of the Li^+ cation is lower than the mobility of the Na^+ cation, due to the smaller ionic radius of the former and its stronger interaction with the anionic species in these melts. Therefore, the specific electrical conductivity of the $\text{AlCl}_3\text{-LiCl}$ melts is lower by approximately 20% at the corresponding compositions. This will be discussed in more detail in Section 3.2 of this Report. However, there is no appreciable difference in the electrochemical span of the two binary melt systems, since their limiting cathodic potentials are determined by the aluminum deposition process,

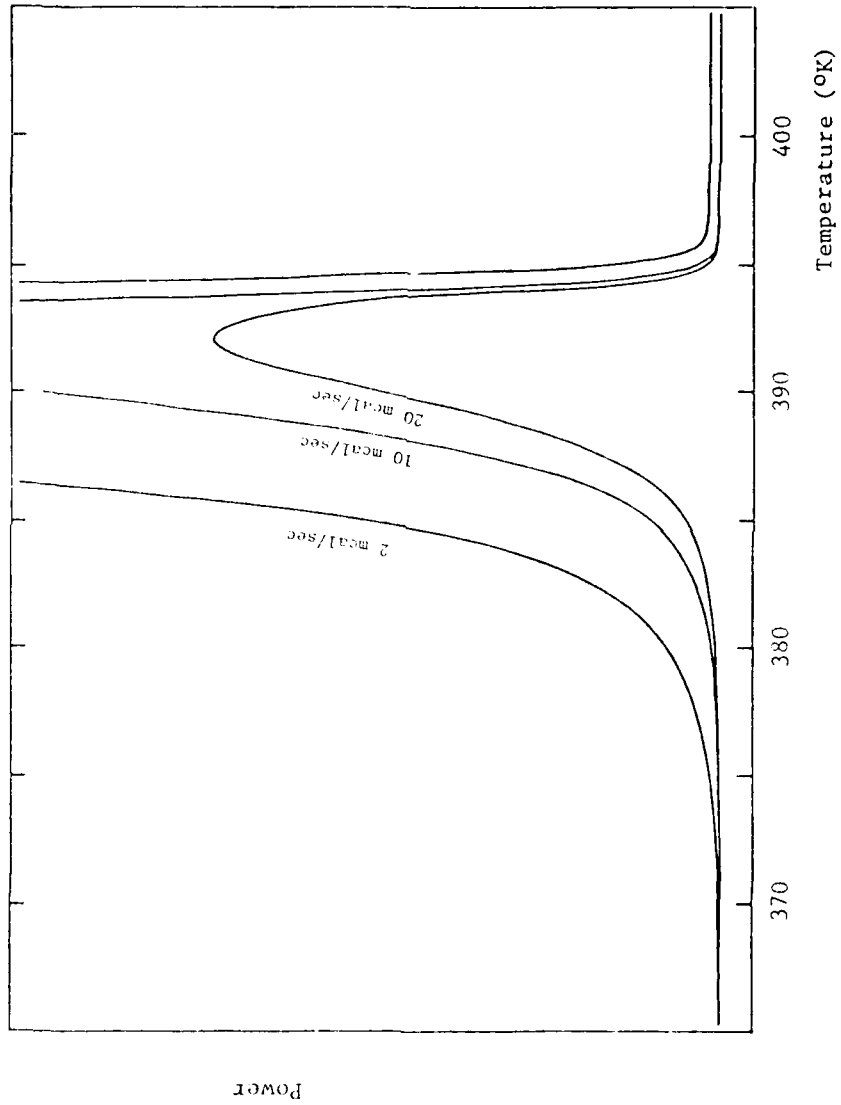


Figure 1. DSC Recordings of 61.0-39.0 Mole % AlCl_3 -NaCl at Sensitivity of 2, 10, and 20 mcal/sec Full Scale.

and not by the alkali metal deposition.

The two binary aluminum chloride-alkali chloride systems have been extensively studied (4,12,13). No phase diagram data, however, are available in the literature for the AlCl_3 -LiCl-NaCl ternary system. The latter is presently being studied at F. J. Seiler Research Laboratory (17). Their results, combined with our data, will provide a detailed description of the low melting composition region of the phase diagram of this important ternary system.

Our data for the three sections of the AlCl_3 -LiCl-NaCl system are shown in Table 1.1. The LiCl to NaCl mole ratio in these sections was maintained constant, 3 to 1, 1 to 1, and 1 to 3, respectively. Two of these sections are also shown in Figure 2. The least squares fitting of these data, as well as of the data from EJSRL, has not yet been performed, and only a brief qualitative discussion of our experimental results will be given here.

The liquidus curves of the two sections of the AlCl_3 -LiCl-NaCl ternary system resemble the liquidus curve of the AlCl_3 -NaCl system. Their minima are displaced towards the alkali chloride rich compositions with respect to the eutectic composition of the AlCl_3 -NaCl system. This displacement is as much as ca. 5.5 mole % of AlCl_3 for the 1 to 1 LiCl to NaCl section. The latter also exhibits the lowest liquidus temperatures. In view of the similarity of the two alkali cations, as well as of the AlCl_3 -LiCl and AlCl_3 -NaCl binary systems, the similarity of the liquidus curves of the three studied sections seems reasonable. The solidus temperature of all three sections is the same, and is lowered by ca. 30°C with respect to the AlCl_3 -NaCl solidus temperature.

2.4. Other Ternary AlCl_3 -NaCl Systems

We have performed preliminary measurements on two other ternary aluminum chloride-alkali chloride systems: the AlCl_3 -NaCl-KCl system and the AlCl_3 -LiCl-KCl system. Our results (Table 1.2) indicate that the solidus temperatures of these two systems, ca. 100°C for the former, and ca. 98°C for the latter, are quite close to each other. The literature value of 93°C for the ternary eutectic temperature of the AlCl_3 -NaCl-KCl system (18) is low in comparison to our value. Other reported values (cf. references in 18) are even lower and are probably incorrect.

The phase diagram of the AlCl_3 -LiCl-KCl system is available in the literature (19). The reported ternary eutectic temperature of 84-85°C seems also too low in comparison to our value of ca. 98°C. Our liquidus temperature data are also not in good agreement with the literature values. Considerably more work is required if the source of these disagreements is to be clarified.

2.5. AlCl_3 - BaCl_2 -NaCl System

The complete phase diagram of the AlCl_3 - BaCl_2 -NaCl ternary system has been studied recently (20). The melting point of 50°C has been reported for the ternary eutectic with the composition of 63.6-2.6-33.8 mole % (20). Since

Table 1

Phase Diagram Data for AlCl_3 -LiCl-NaCl System

Composition (Mole %)			Solidus Temperature (°C)	Liquidus Temperature (°C)
AlCl_3	LiCl	NaCl		
52.0	24.0	24.0	86	105
54.0	23.0	23.0	86	101
56.0	22.0	22.0	86	96
58.0	21.0	21.0	86	100.5
60.0	20.0	20.0	86	124
62.0	19.0	19.0	86	136.5
68.0	16.0	16.0	86	168
53.4	35.0	11.6	86	119
56.0	33.0	11.0	86	112
58.0	31.5	10.5	86	105
60.0	30.0	10.0	86	107
68.0	24.0	8.0	86	172
52.0	12.0	36.0	86	128
56.0	11.0	33.0	86	110
59.0	10.2	30.8	86	105
62.0	9.5	28.5	86	105
55.0	27.5	17.5	86	103

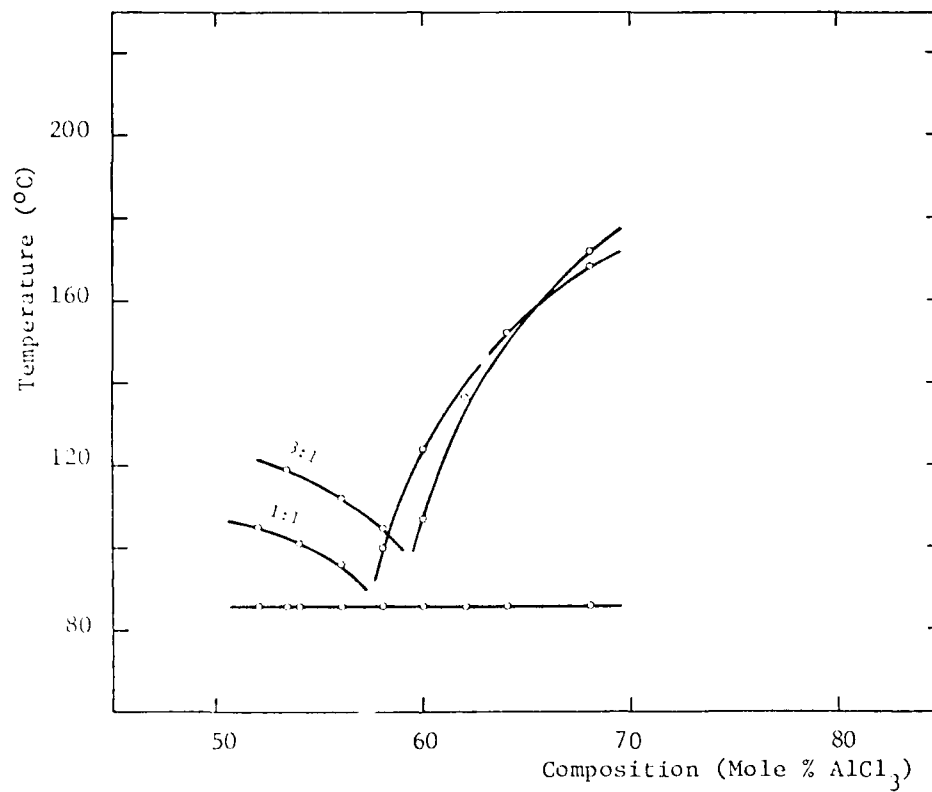


Figure 2. Phase Diagram Data for AlCl₃-LiCl-NaCl System. LiCl to NaCl mole ratios are indicated on the liquidus curves.

Table 2.

Phase Diagram Data for Other Ternary Alkali
Chloroaluminate Systems

Composition (mole %)			Solidus Temperature (°C)	Liquidus Temperature (°C)
AlCl ₃	NaCl	KCl		
55.0	31.6	13.4	100	118
61.2	24.8	14.0	100	108
63.4	22.4	14.2	101	147
AlCl ₃	LiCl	KCl		
51.2	35.8	13.0	98	118
60.8	25.8	13.4	98	167

this is the lowest liquidus temperature reported to date for an inorganic chloroaluminate melt, it was of interest to verify the information.

The results of our DSC measurements are shown in Table 1.3. One of our samples was prepared to have exactly the same composition as quoted in the literature for the lowest melting ternary eutectic; only the mole fraction of AlCl_3 was varied in the other two. Thus the BaCl_2 to NaCl mole ratio was the same in all three samples.

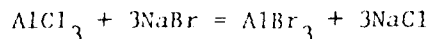
Our results do not reproduce the above literature data. Our sample with the 63.6-2.6-33.8 mole % composition has the liquidus range of ca. 25°C , which indicates that the true eutectic composition is quite far from the cited composition. The 60.0-2.9-37.1 mole % sample, with the liquidus range of ca. 10°C , is much closer to the true eutectic point. We do not observe any phase transitions below 108°C . Since our results demonstrate that the addition of BaCl_2 lowers the solidus temperature of the AlCl_3 - NaCl binary system by only 7°C , and does not change appreciably the liquidus temperatures at the studied compositions, the effect of BaCl_2 as an additive is marginal. In view of this result, a further study of this system is probably not justified.

2.6. AlCl_3 - CaCl_2 - NaCl System

No data are available in the literature for the AlCl_3 - CaCl_2 - NaCl system. Our DSC data for the samples with compositions similar to the AlCl_3 - BaCl_2 - NaCl compositions are shown in Table 1.4. These results indicate that the solidus temperature in the AlCl_3 - CaCl_2 - NaCl system is 108°C . The liquidus temperatures of the studied samples with CaCl_2 are very close to the liquidus temperatures of the corresponding AlCl_3 - BaCl_2 - NaCl samples, and therefore to the liquidus temperatures of the binary AlCl_3 - NaCl system at the same mole fraction of AlCl_3 . Perhaps not unexpectedly, CaCl_2 and BaCl_2 have qualitatively the same effect on the AlCl_3 - NaCl system. In short, the effect of CaCl_2 is not spectacular, and it does not seem very useful to pursue further measurements on this system.

2.7 AlCl_3 - NaBr System

In order to find out whether the liquidus range of chloroaluminate melts will be significantly lowered by the presence of a second halide ion, the AlCl_3 - NaBr system has been studied. This system is a section of the more complex AlCl_3 - AlBr_3 - NaCl - NaBr system. The latter is still only a ternary system, since its four components are related by the equilibrium



and its nominal composition can be expressed in terms of only three of its components. Therefore, the mole percentages of only one cation and one anion are sufficient to define the total nominal composition of the system. No phase diagram data are available in the literature for these systems.

Table 3.

Phase Diagram Data for AlCl_3 - BaCl_2 - NaCl System

Composition (Mole %)			Solidus Temperature (°C)	Liquidus Temperature (°C)
AlCl_3	BaCl_2	NaCl		
56.0	3.2	40.8	108	136
60.0	2.9	37.1	108	118
63.6	2.6	33.8	108	134

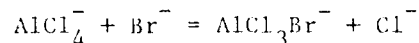
Table 4.

Phase Diagram Data for AlCl_3 - CaCl_2 - NaCl System

Composition (Mole %)			Solidus Temperature (°C)	Liquidus Temperature (°C)
AlCl_3	CaCl_2	NaCl		
56.0	3.7	40.3	108	136
60.0	3.3	36.7	108	121
64.0	3.0	33.0	107	137.5

Table 1.5 and Figure 3 show our liquidus temperature data for the $\text{AlCl}_3\text{-NaBr}$ system. The literature data for the $\text{AlCl}_3\text{-NaCl}$ system (12) and for the $\text{AlBr}_3\text{-NaBr}$ system (12) are also shown in this figure. Three features of the $\text{AlCl}_3\text{-NaBr}$ data are noticeable:

1. The liquidus curve for the $\text{AlBr}_3\text{-NaCl}_3$ system strongly resembles the $\text{AlCl}_3\text{-NaCl}$ liquidus curve. Both have only one eutectic point in the low melting composition region, the $\text{AlCl}_3\text{-NaBr}$ system at ca. 62 mole % AlCl_3 , which is very close to the composition of the $\text{AlCl}_3\text{-NaCl}$ eutectic of 61.4 mole % AlCl_3 . On the other hand, the $\text{AlBr}_3\text{-NaBr}$ system has three minima at ca. 68, 78 and 81 mole % AlBr_3 due to the existence of several compounds stable in the solid phase. Phase diagrams of the other alkali bromide-aluminum bromide systems also exhibit at least two minima (21,22).
2. The liquidus curve for the $\text{AlCl}_3\text{-NaBr}$ system is depressed by as much as approximately 20°C with respect to the $\text{AlCl}_3\text{-NaCl}$ system.
3. The solidus temperature of the $\text{AlCl}_3\text{-NaBr}$ system is not independent of the composition. It gradually decreases from 86°C at 28 mole % NaBr to 72°C at 48 mole % NaBr . This effect is possibly due to the exchange of the Cl^- and Br^- ions in the haloaluminate species:



This significant gain in the lowering of the liquidus range of the $\text{AlCl}_3\text{-NaBr}$ system is partially offset by a probable reduction in the specific electrical conductivity as well as the narrowing of the electrochemical span compared to the $\text{AlCl}_3\text{-NaCl}$ system. No conductivity data are available for the mixed chloride-bromide system. The conductivity in the pure bromide system $\text{AlBr}_3\text{-NaBr}$ is considerably lower than the conductivity of the $\text{AlCl}_3\text{-NaCl}$ system at the corresponding compositions (23). Perhaps the conductivity loss in the mixed chloride-bromide system will not be so severe.

Data on the electrochemical span in the mixed chloride-bromide melts are available in literature. The bromine evolution potential has been reported as +1.61 V relative to the Al(III)-Al(0) reference potential (24), which should be compared to + 2.09 V for the chlorine evolution potential in the $\text{AlCl}_3\text{-NaCl}$ system. The data for the $\text{AlCl}_3\text{-NaBr-KBr}$ melts show a potential of 1.71 V (24), which has been attributed to the mixed chlorine-bromine evolution. Thus the reduction of the electrochemical span in the mixed chloride-bromide systems amounts to 0.4 to 0.5 V.

2.8. $\text{AlBr}_3\text{-R}_4\text{NBr}$ Systems

The low melting points of the pure quaternary ammonium halides, (74-420°C range, except for the tetramethyl and tetraethyl bromides which decompose before melting) as well as the chemical stability of their cations, give rise to expectations that the aluminum halide-quaternary ammonium halide molten salt systems may be low melting solvents of considerable promise for the battery applications. The quaternary ammonium cations, being basic, a.

Table 5.

Phase Diagram Data for AlCl_3 -NaBr System

Composition (Mole %)		Solidus Temperature (°C)	Liquidus Temperature (°C)
AlCl_3	NaBr		
52.0	48.0	72	127
56.0	44.0	80	117.5
60.0	40.0	80	100
64.0	36.0	83	112
68.0	32.0	85	146
72.0	28.0	86	165

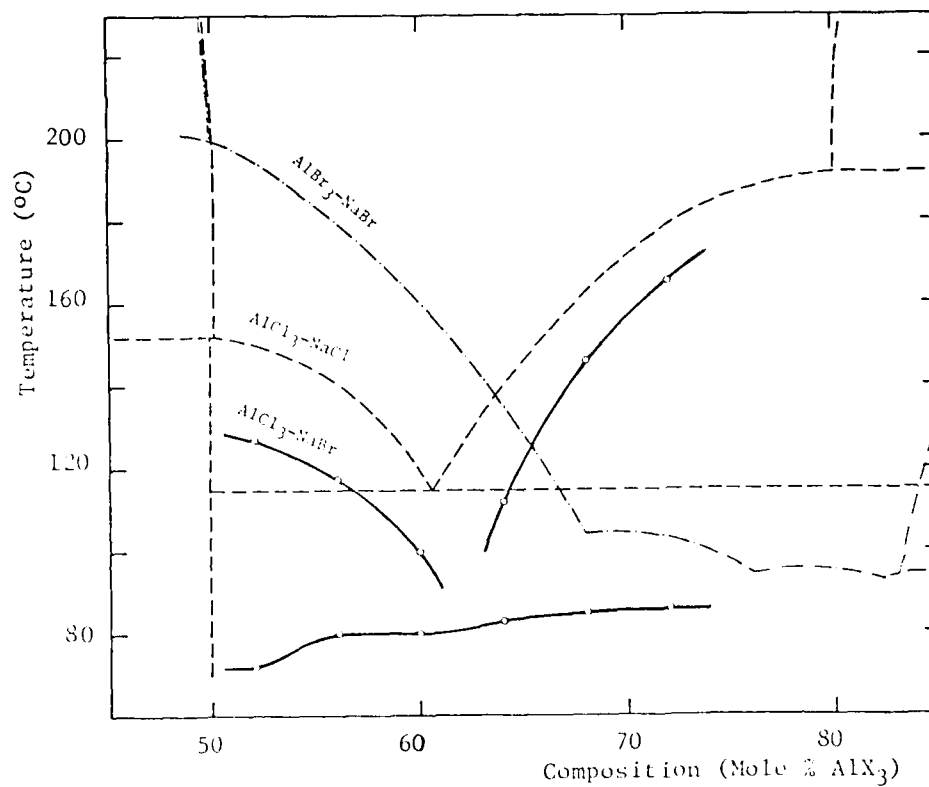


Figure 3. Phase Diagrams of AlCl₃-NaBr, AlCl₃-NaCl (12), and AlBr₃-NaBr (12) Systems.

well as chemically very stable due to the saturated character of their bonding, have similarities with the alkali cations. However, the large ionic radius of even the smallest of the quaternary ammonium cations, the tetramethyl ammonium ion, introduces a significant new factor in the structure of their haloaluminates, and thus influences the physical and chemical properties, such as the electrical conductivity, of the quaternary ammonium haloaluminate melts. Also, the expected structural differences in the solid phase, due to the size of their cations, make it difficult to predict the shape of their phase diagrams. The aluminum halide-quaternary ammonium halide molten salt systems have not been studied to date.

We are studying two quaternary ammonium bromoaluminate systems at present: $\text{AlBr}_3\text{-Bu}_4\text{NBr}$, and $\text{AlBr}_3\text{-Me}_4\text{NBr}$. The bromide were chosen to start with, since the quaternary ammonium chlorides are more difficult to prepare in the anhydrous form than the bromides. Since it is not clear at this point how reproducible are our preliminary data, only a qualitative discussion of our results will be given.

2.9. $\text{AlBr}_3\text{-Bu}_4\text{NBr}$ System

This system appears to be thermally stable below ca. 140°C for extended periods of time (No observable changes for periods up to 3 weeks.)

The melts in the 60.0 to 70.0 mole % of Bu_4NBr range are liquid at the room temperature. This is a most important finding. It also indicates that the solidus temperature of all the melts in the Bu_4NBr rich composition region is probably below the room temperature as well. The appearance of a liquid phase was observed in most of the $\text{AlBr}_3\text{-Bu}_4\text{NBr}$ freshly prepared samples before melting in the furnace. However, the solidus temperature of these samples was too low to be verified with our DSC-1B instrument. The solidus temperature(s) of the AlBr_3 rich composition, are in the $60\text{-}70^\circ\text{C}$ range.

2.10. $\text{AlBr}_3\text{-Me}_4\text{NBr}$ System

In view of the smaller size of the Me_4N^+ ion compared to the Bu_4N^+ ion, the $\text{AlBr}_3\text{-Me}_4\text{NBr}$ system is probably the more interesting of the two molten salt systems. This system is also thermally stable below ca. $130\text{-}140^\circ\text{C}$ for extended periods of time. As was the case with the $\text{AlBr}_3\text{-Bu}_4\text{NBr}$ system, the AlBr_3 rich composition region of the $\text{AlBr}_3\text{-Me}_4\text{NBr}$ system is also not very low melting, since its solidus temperature is in the $70\text{-}80^\circ\text{C}$ range. However, the major difference between the two quaternary ammonium bromoaluminate systems is that the Me_4NBr rich composition region of the $\text{AlBr}_3\text{-Me}_4\text{NBr}$ system does not melt completely even up to 230°C , which is the decomposition temperature of the pure Me_4NBr . If this finding is verified in our further experiments, the $\text{AlBr}_3\text{-Me}_4\text{NBr}$ system may not be as promising as it was originally expected to be.

It should be noted here that the DSC-1B instrument used in our studies is not suitable for the low temperature work. Although its temperature range

can be extended down to 0°C with the aid of a liquid nitrogen dewar type cover for its furnace, the instrument does not perform very satisfactorily in this temperature range, nor is it able to maintain these temperatures for an extended time. We plan to rely more on the visual observation of samples sealed in Pyrex in a very slowly heated silicone oil thermostat bath in the future work.

3. ELECTRICAL CONDUCTIVITY STUDIES

3.1. Experimental

The specific electrical conductivity measurements were performed by the conventional AC method. The equipment consisted of a Hewlett-Packard wide band oscillator Model 200 CD, an RC bridge built in our electronics shop, General Radio precision decade resistors and capacitors and a Tektronix Model 549 oscilloscope. The furnace with an aluminum block body and non-inductive cartridge heaters was controlled by a proportional controller also built in our electronics shop; the temperature of the cell was read with a chromel-alumel thermocouple and a Fluke Model 895 DC differential voltmeter.

A small volume capillary conductivity cell with platinum foil electrodes was built of Pyrex (Figure 4). It was calibrated at 25°C with the 1 demal KCl solution according to the standard procedure of Jones and Bradshaw (25). The value of the cell constant was 218.93 cm^{-1} , and the measured resistances were in the 300-1500 ohm range. The calculated temperature dependence of the cell constant was of the order of $0.00015 \text{ cm}^{-1}\text{deg}^{-1}$. Since the calculated change of the cell constant over the 300°C temperature range was only 0.05 cm^{-1} , it was ignored in further work.

The measurements were performed at the frequency of 1.0 kHz. The frequency dispersion of the melts was not studied, since the temperature of the furnace was not sufficiently stable to permit the retuning of the RC bridge for different frequencies.

The conductivity equipment is currently being improved by the addition of a large volume silicone oil constant temperature bath and a Bayley Model 124 proportional temperature controller. This setup is expected to provide the temperature stability of the order of $\pm 0.01^\circ\text{C}$.

3.2. AlCl_3 -LiCl-NaCl System

No electrical conductivity data are available in the literature for the AlCl_3 -LiCl-NaCl molten salt system. However, the work on this system is also in progress at the E. J. Seiler Research Laboratory (27).

Our specific conductivity measurements on the AlCl_3 -LiCl-NaCl system were performed in the temperature range from the melting point of the samples to 300°C. In the very acidic melts, which have considerable vapor pressure, the upper temperature limit was lowered accordingly. The same samples which were used for the liquidus range studies were also used for the conductivity

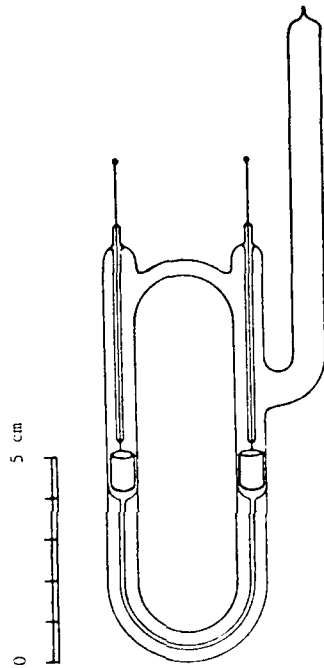


Figure 4. Electrical Conductivity Cell.

work. The reproducibility of the data was checked by performing measurements on two different samples of the 54.0-23.0-23.0 mole % melt. The agreement of the measured conductivities was within 0.25% and was probably limited by the reproducibility of the sample compositions.

Our data for the AlCl_3 -LiCl-NaCl system are listed in Tables 2.1 to 2.13 and the specific conductivity vs. temperature plots are shown in Figures 5 and 6. The data were fitted by the least squares method to a polynomial equation of the second order in temperature:

$$\kappa = A_0 + A_1T + A_2T^2 \quad (1)$$

where κ is the specific conductivity in $\text{ohm}^{-1}\text{cm}^{-1}$, and T is the absolute temperature. The coefficients A_0 , A_1 and A_2 are listed in Table 3. The second order coefficient A_2 is a measure of the curvature of the conductivity vs. temperature plots.

Table 3 and Figures 5 and 6 indicate that the curvature of the conductivity vs. temperature plots becomes more positive with the increasing mole fraction of AlCl_3 in the melts. This may be due, in part, to the increasing volatility of AlCl_3 in the acidic melts. The loss of AlCl_3 from the molten phase effectively increases the concentration of the two alkali chlorides, and therefore of the Li^+ and Na^+ cations, which are the dominant conducting species in the chloroaluminate melts.

A comparison of the conductivity of the melts with the same AlCl_3 mole fraction, but different LiCl to NaCl mole ratio is not very revealing. The specific conductivity of the melts with 3:1 LiCl to NaCl mole ratio is consistently lower than the conductivity of the corresponding 1:1 melts. In the most acidic melts this difference is about 10%. This is in agreement with the lower ionic mobility of the Li^+ ion compared to the mobility of the Na^+ ion, both in the aqueous solutions (26) and in the binary chloroaluminate melts, and is probably due to the more covalent character of the interaction of the Li^+ cation with the other species in these melts.

The conductivity data for two compositions may require further study. The curvature of the conductivity vs. temperature curve for the 62.0-19.0-19.0 mole % melt is clearly out of sequence (Table 3). The conductivity curve for the 60.0-20.0-20.0 mole % melt, on the other hand, has a barely discernible break at ca. 200°C (Figure 5). This results in the apparently larger curvature than the curvature of either section of the conductivity vs. temperature plot for this composition.

3.3. Measurements in the Solid Phase

AC conductivity in the solid phase was used as an alternate technique to study the solid-liquid phase transitions of some AlCl_3 -NaCl and AlCl_3 -LiCl-NaCl samples. The measurements were performed with the same equipment used for the molten salt conductivity studies, except for the conductivity cell, which was of the conventional low resistance liquid type. The molten samples were frozen in the cell by quenching in the ice-water bath, and then annealed

work. The reproducibility of the data was checked by performing measurements on two different samples of the 54.0-23.0-23.0 mole % melt. The agreement of the measured conductivities was within 0.25% and was probably limited by the reproducibility of the sample compositions.

Our data for the AlCl_3 -LiCl-NaCl system are listed in Tables 2.1 to 2.13 and the specific conductivity vs. temperature plots are shown in Figures 5 and 6. The data were fitted by the least squares method to a polynomial equation of the second order in temperature:

$$\kappa = A_0 + A_1T + A_2T^2 \quad (1)$$

where κ is the specific conductivity in $\text{ohm}^{-1}\text{cm}^{-1}$, and T is the absolute temperature. The coefficients A_0 , A_1 and A_2 are listed in Table 3. The second order coefficient A_2 is a measure of the curvature of the conductivity vs. temperature plots.

Table 3 and Figures 5 and 6 indicate that the curvature of the conductivity vs. temperature plots becomes more positive with the increasing mole fraction of AlCl_3 in the melts. This may be due, in part, to the increasing volatility of AlCl_3 in the acidic melts. The loss of AlCl_3 from the molten phase effectively increases the concentration of the two alkali chlorides, and therefore of the Li^+ and Na^+ cations, which are the dominant conducting species in the chloroaluminate melts.

A comparison of the conductivity of the melts with the same AlCl_3 mole fraction, but different LiCl to NaCl mole ratio is not very revealing. The specific conductivity of the melts with 3:1 LiCl to NaCl mole ratio is consistently lower than the conductivity of the corresponding 1:1 melts. In the most acidic melts this difference is about 10%. This is in agreement with the lower ionic mobility of the Li^+ ion compared to the mobility of the Na^+ ion, both in the aqueous solutions (26) and in the binary chloroaluminate melts, and is probably due to the more covalent character of the interaction of the Li^+ cation with the other species in these melts.

The conductivity data for two compositions may require further study. The curvature of the conductivity vs. temperature curve for the 62.0-19.0-19.0 mole % melt is clearly out of sequence (Table 3). The conductivity curve for the 60.0-20.0-20.0 mole % melt, on the other hand, has a barely discernible break at ca. 200°C (Figure 5). This results in the apparently larger curvature than the curvature of either section of the conductivity vs. temperature plot for this composition.

3.3. Measurements in the Solid Phase

AC conductivity in the solid phase was used as an alternate technique to study the solid-liquid phase transitions of some AlCl_3 -NaCl and AlCl_3 -LiCl-NaCl samples. The measurements were performed with the same equipment used for the molten salt conductivity studies, except for the conductivity cell, which was of the conventional low resistance liquid type. The molten samples were frozen in the cell by quenching in the ice-water bath, and then annealed

Table 6.

Specific Conductivity Data for AlCl_3 -LiCl-NaCl System at 1.0 KHz

Composition: 52.0 - 24.0 - 24.0 (Mole %)

Temperature (°C)	Specific Conductivity ($\text{ohm}^{-1}\text{cm}^{-1}$)
120	0.2377*
130	0.2637*
140	0.2894*
150	0.3155
160	0.3400
170	0.3645
180	0.3889
190	0.4129
200	0.4370
210	0.4608
220	0.4844
230	0.5075
240	0.5298
250	0.5522
260	0.5743
270	0.5956
279.3	0.6162
290	0.6377
298.3	0.6549

* Calculated from Eqn. 1

Table 7.

Specific Conductivity Data for AlCl_3 -LiCl-NaCl System at 1.0 KHz

Composition: 54.0 - 23.0 - 23.0 (Mole %)

Temperature (°C)	Specific Conductivity ($\text{ohm}^{-1}\text{cm}^{-1}$)
110	0.1895
119.2	0.2122
130	0.2344
140	0.2568
150	0.2794
159.3	0.3002
170	0.3240
182.5	0.3519
190	0.3690
200	0.3909
210	0.4120
220	0.4333
230	0.4545
240	0.4754
250	0.4959
261	0.5183
270	0.5362
280	0.5558
290	0.5752
300	0.5944

Table 8.
 Specific Conductivity Data for $\text{AlCl}_3 \cdot \text{LiCl-NaCl}$ System at 1.0 KHz
 Composition: 56.0 - 22.0 - 22.0 (Mole %)

Temperature (°C)	Specific Conductivity ($\text{ohm}^{-1}\text{cm}^{-1}$)
100	0.1404*
110	0.1620*
120	0.1835*
130	0.2048*
140	0.2265
150.7	0.2483
160	0.2674
170	0.2881*
180	0.3081
190	0.3285
200	0.3486
210	0.3684
220	0.3882
231	0.4097
240	0.4271
250	0.4464
260.6	0.4667
269.8	0.4840
280	0.5027
290	0.5200
300	0.5387

* Calculated from Eqn. 1

Table 9.

Specific Conductivity Data for AlCl_3 -LiCl-NaCl System at 1.0 KHz

Composition: 58.0 - 21.0 - 21.0 (Mole %)

Temperature (°C)	Specific Conductivity ($\text{ohm}^{-1}\text{cm}^{-1}$)
120	0.1629*
130	0.1821*
140	0.2023
150	0.2196
160	0.2378
170	0.2568
180	0.2755
190	0.2939
200	0.3121
210	0.3301
220	0.3480
230	0.3657
240	0.3832
250	0.4005
260	0.4178
270	0.4346
280	0.4517
290	0.4683
300	0.4847

* Calculated from Eqn. 1

Table 10.

Specific Conductivity Data for AlCl_3 -LiCl-NaCl System at 1.0 KHz

Composition: 60.0 - 20.0 - 20.0 (Mole %)

Temperature (°C)	Specific Conductivity ($\text{ohm}^{-1}\text{cm}^{-1}$)
130	0.1667*
140	0.1837*
150	0.2009
160	0.2175
170	0.2351
180	0.2523
190	0.2683
200	0.2862*
210	0.3036
220	0.3202
230	0.3373
239.9	0.3553
250	0.3728*
259.4	0.3905
270	0.4085
280	0.4256
290	0.4424
300	0.4601

* Calculated from Eqn. 1

Table 11.

Specific Conductivity Data for AlCl_3 -LiCl-NaCl System at 1.0 KHz

Composition: 62.0 - 19.0 - 19.0 (Mole %)

Temperature (°C)	Specific Conductivity ($\text{ohm}^{-1}\text{cm}^{-1}$)
150	0.1783
160	0.1940
170	0.2101
180	0.2259
190	0.2417
200	0.2581
210	0.2747
220	0.2915
230	0.3090
240	0.3256
250	0.3432
260	0.3587
270	0.3755
280	0.3925
290	0.4095
300	0.4254

Table 12.

Specific Conductivity Data for AlCl_3 -LiCl-NaCl System at 1.0 KHz

Composition: 64.0 - 18.0 - 18.0 (Mole %)

Temperature (°C)	Specific Conductivity ($\text{ohm}^{-1}\text{cm}^{-1}$)
160	0.1801*
170	0.1941*
181.4	0.2098
190.8	0.2231
200	0.2360
210	0.2503
219.8	0.2641
230.6	0.2791
241	0.2934
250	0.3069
260	0.3208
269.8	0.3349

* Calculated from Eqn 1

Table 13.

Specific Conductivity Data for AlCl_3 -LiCl-NaCl System at 1.0 KHz

Composition: 68.0 - 16.0 - 16.0 (Mole %)

Temperature (°C)	Specific Conductivity ($\text{ohm}^{-1}\text{cm}^{-1}$)
180	0.1790
190	0.1907
200	0.2027
210	0.2134
220	0.2250
230	0.2368
240	0.2482
250	0.2603

Table 14.

Specific Conductivity Data for AlCl_3 -LiCl-NaCl System at 1.0 KHz

Composition: 53.4 - 35.0 - 11.6 (Mole %)

Temperature (°C)	Specific Conductivity ($\text{ohm}^{-1}\text{cm}^{-1}$)
130	0.2283
140	0.2506
150	0.2730
160	0.2949
170	0.3170
180	0.3385
190	0.3607
200	0.3825*
210	0.4038
220	0.4250
230	0.4462
240	0.4666
249.8	0.4868
260	0.5074
270	0.5270
280	0.5464
290	0.5654
300	0.5854*

* Calculated from Eqn. 1.

Table 15.

Specific Conductivity Data for AlCl_3 -LiCl-NaCl System at 1.0 KHz

Composition: 56.0 - 33.0 - 11.0 (Mole %)

Temperature (°C)	Specific Conductivity ($\text{ohm}^{-1}\text{cm}^{-1}$)
130	0.1912*
140	0.2116*
151	0.2338
160.8	0.2534
170	0.2717
180	0.2914
190	0.3111
200	0.3301
210	0.3497
220	0.3688
230	0.3869
240	0.4053
251.9	0.4273
261	0.4436
270	0.4599
280	0.4779
290	0.4955
300	0.5126

* Calculated from Eqn. 1.

Table 16.

Specific Conductivity Data for AlCl_3 -LiCl-NaCl System at 1.0 KHz

Composition: 58.0 - 31.5 - 10.5 (Mole %)

Temperature (°C)	Specific Conductivity ($\text{ohm}^{-1}\text{cm}^{-1}$)
120	0.1526*
130	0.1711*
140	0.1902
150	0.2076
160	0.2255
170	0.2435
180	0.2612
190	0.2792
200	0.2968
209.9	0.3139
220.2	0.3316
230	0.3497
240	0.3667
250	0.3832
260	0.4002
270	0.4172
281	0.4348
292.7	0.4543
301.6	0.4689

* Calculated from Eqn. 1.

Table 17.

Specific Conductivity Data for AlCl_3 -LiCl-NaCl System at 1.0 KHz

Composition: 60.0 - 30.0 - 10.0 (Mole %)

Temperature (°C)	Specific Conductivity ($\text{ohm}^{-1}\text{cm}^{-1}$)
120	0.1389*
131	0.1571
140.3	0.1719
150	0.1874
159.8	0.2035
171	0.2217
180	0.2362
190	0.2526
200	0.2687
210	0.2847
222.6	0.3048
230	0.3162
240	0.3321
250	0.3481
260	0.3639
271	0.3812
280	0.3957*
290	0.4120
300	0.4269

* Calculated from Eqn. 1.

Table 18.

Specific Conductivity Data for AlCl_3 -LiCl-NaCl System at 1.0 KHz

Composition: 68.0 - 24.0 - 8.0 (Mole %)

Temperature (°C)	Specific Conductivity ($\text{ohm}^{-1}\text{cm}^{-1}$)
170	0.1571*
180	0.1681*
190	0.1791*
200	0.1898
210	0.2011
220.3	0.2121
230	0.2228
240	0.2336
250	0.2446

* Calculated from Eqn. 1.

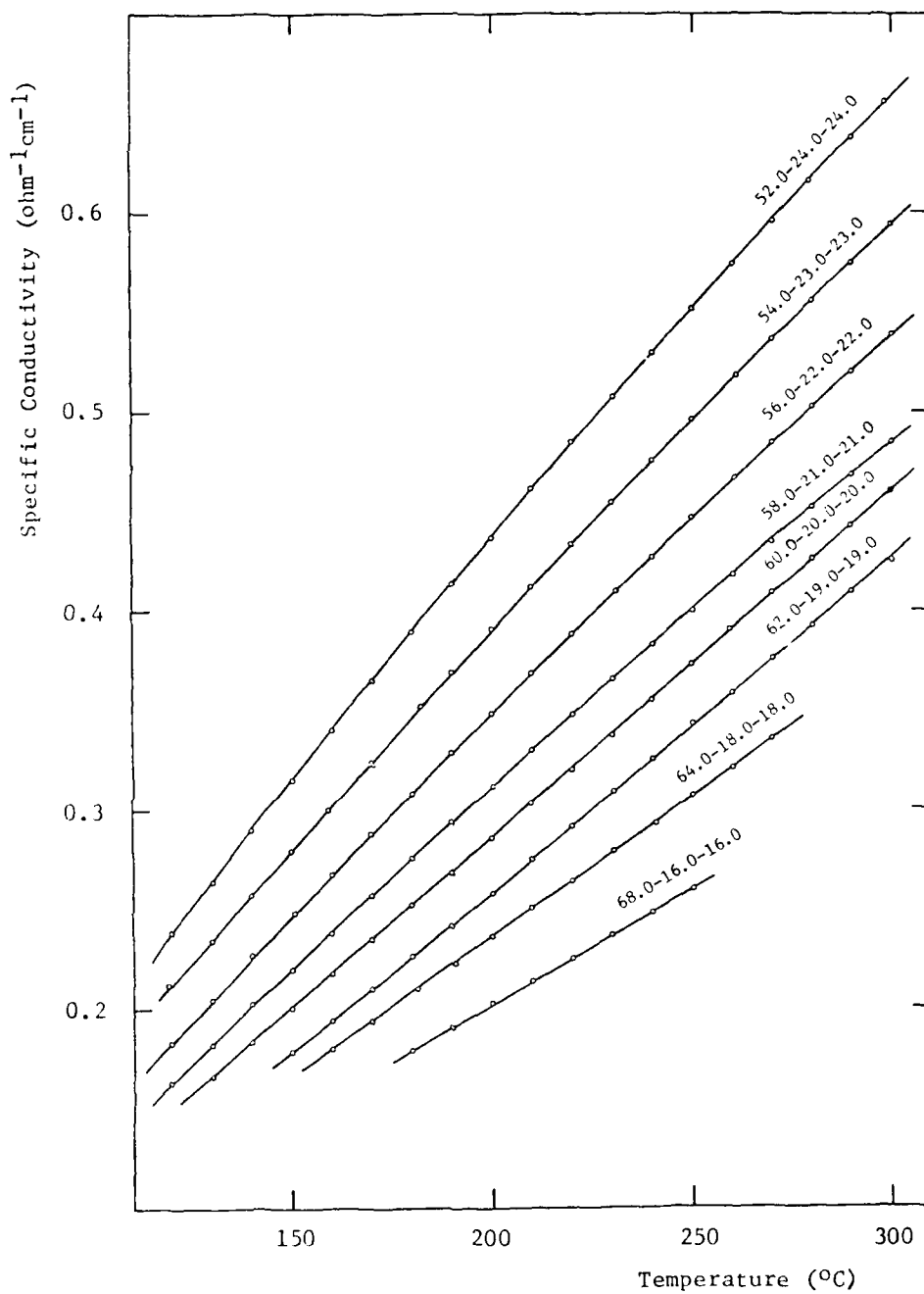


Figure 5. Specific Conductivity of AlCl_3 - LiCl - NaCl System (LiCl-NaCl Mole Ratio 1:1). Composition in mole % is indicated on the curves.

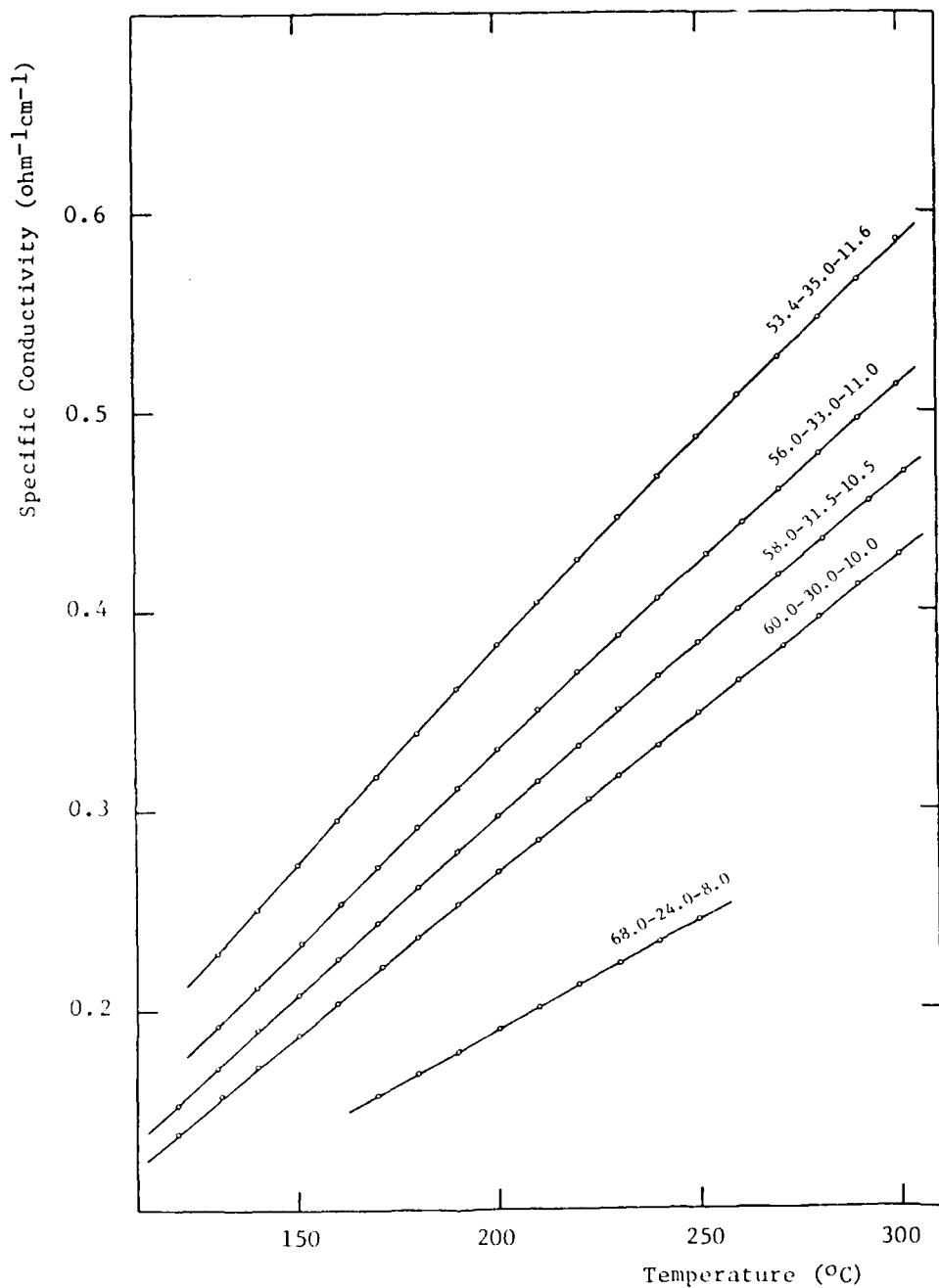


Figure 6. Specific Conductivity of AlCl₃-LiCl-NaCl System (LiCl-NaCl Mole Ratio 3:1). Composition in mole % is indicated on the curves.

Table 19.

Temperature Dependence of the Specific Conductivity of the
AlCl₃-LiCl-NaCl System

Composition (Mole %)			Coefficients for Equation 1		
AlCl ₃	LiCl	NaCl	A ₀	A ₁ × 10 ³	A ₂ × 10 ⁶
(LiCl-NaCl Mole Ratio 1:1)					
52.0	24.0	24.0	-1.02747	3.81867	-1.52860
54.0	23.0	23.0	-0.84931	3.09007	-0.99411
56.0	22.0	22.0	-0.79713	2.85035	-0.90625
58.0	21.0	21.0	-0.70954	2.51345	-0.74940
60.0	20.0	20.0	-0.48036	1.51815	0.21516
62.0	19.0	19.0	-0.44525	1.33423	0.32510
64.0	18.0	18.0	-0.39984	1.28372	0.12712
68.0	16.0	16.0	-0.30053	0.96894	0.19290
(LiCl-NaCl Mole Ratio 3:1)					
53.4	35.0	11.6	-0.87078	3.15976	-1.08030
56.0	33.0	11.0	-0.79300	2.82780	-0.95952
58.0	31.5	10.5	-0.67084	2.3355-	-0.61367
60.0	30.0	10.0	-0.53101	1.77409	-0.17893
68.0	24.0	8.0	-0.36936	1.27100	-0.18757

prior to the experiment at 10-20°C below the solidus temperature of the sample. Since the high resistance limit of our RC bridge was ca. 10 megohms, the measurements on the solid samples were limited to the temperatures above 75°C for the AlCl₃-NaCl samples and above 55°C for the AlCl₃-LiCl-NaCl samples. A new thin film conductivity cell, which is being built now, is expected to extend the range of measurements towards low temperatures, as well as to improve the uniformity of the temperature within a sample. The heating rate in our experiments was ca. 2.5°C/hr. Both the resistance and the capacitance of solid samples were measured. However, the capacitance was too small to be measured with our RC bridge until a sample was well within its liquidus range.

Our best solid conductivity data are shown in Figure 7. Since our interest was in the shapes of the electrical conductivity vs. temperature curves, the cell used for these measurements was not calibrated, and only the reciprocal resistance is shown on the ordinate axis in this figure. However, the linear, low temperature section of the 1/R curve for the 54.0-23.0-23.0 mole % AlCl₃-LiCl-NaCl sample extrapolates to $1.6 \times 10^{-8} \text{ ohm}^{-1}$ at 25°C. The corresponding value for the same, completely molten, sample at 120°C is $1.6 \times 10^{-2} \text{ ohm}^{-1}$, and its specific conductivity is $0.2120 \text{ ohm}^{-1} \text{ cm}^{-1}$ (Table 2.2). Therefore, the extrapolated specific conductivity of the solid 54.0-23.0-23.0 mole % sample at 25°C is $2.1 \times 10^{-7} \text{ ohm}^{-1} \text{ cm}^{-1}$. Thus it is roughly an order of magnitude higher than our value for the specific conductivity of the solid AlCl₃-NaCl at the same temperature and composition. This is not unexpected in view of the lower solidus temperature of the AlCl₃-LiCl-NaCl. Since these values are extrapolated far beyond the experimentally measured range, they should be accepted with caution.

The shape of the conductivity vs. temperature curves (Figure 7) is difficult to interpret. The conductivity changes by four orders of magnitude in the phase transition, and its temperature dependence drops from 25 deg⁻¹ at 60°C in the solid to 0.19 deg⁻¹ at 120°C in the melt for the 54.0-23.0-23.0 mole % AlCl₃-LiCl-NaCl sample. However, the change is quite gradual and without discontinuities. Both the conductivity and the capacitance assume their quasi-linear shape at ca. 106°C, in agreement with the DSC liquidus data (Table 1.1). On the other hand, the solidus temperature is not well defined. The change of slope of the conductivity curve at ca. 77°C corresponds to the "first deviation from the base line" in the DSC-1B experiments. The experiments on our AlCl₃-NaCl samples performed on the DSC-2 instrument at ORNL, however, have demonstrated that the "first deviation from the baseline" was a function of the sensitivity of the instrument, and thus has little physical significance. The "extrapolated onset" of the steeply rising section of the conductivity curve at 85-86°C corresponds to the "extrapolated onset" on the DSC curve for the 54.0-23.0-23.0 mole % sample. Thus it appears that though both the DSC and conductivity techniques yield information on the same process, the conductivity measurements do not provide an unambiguous independent verification of the solidus temperatures in these melts.

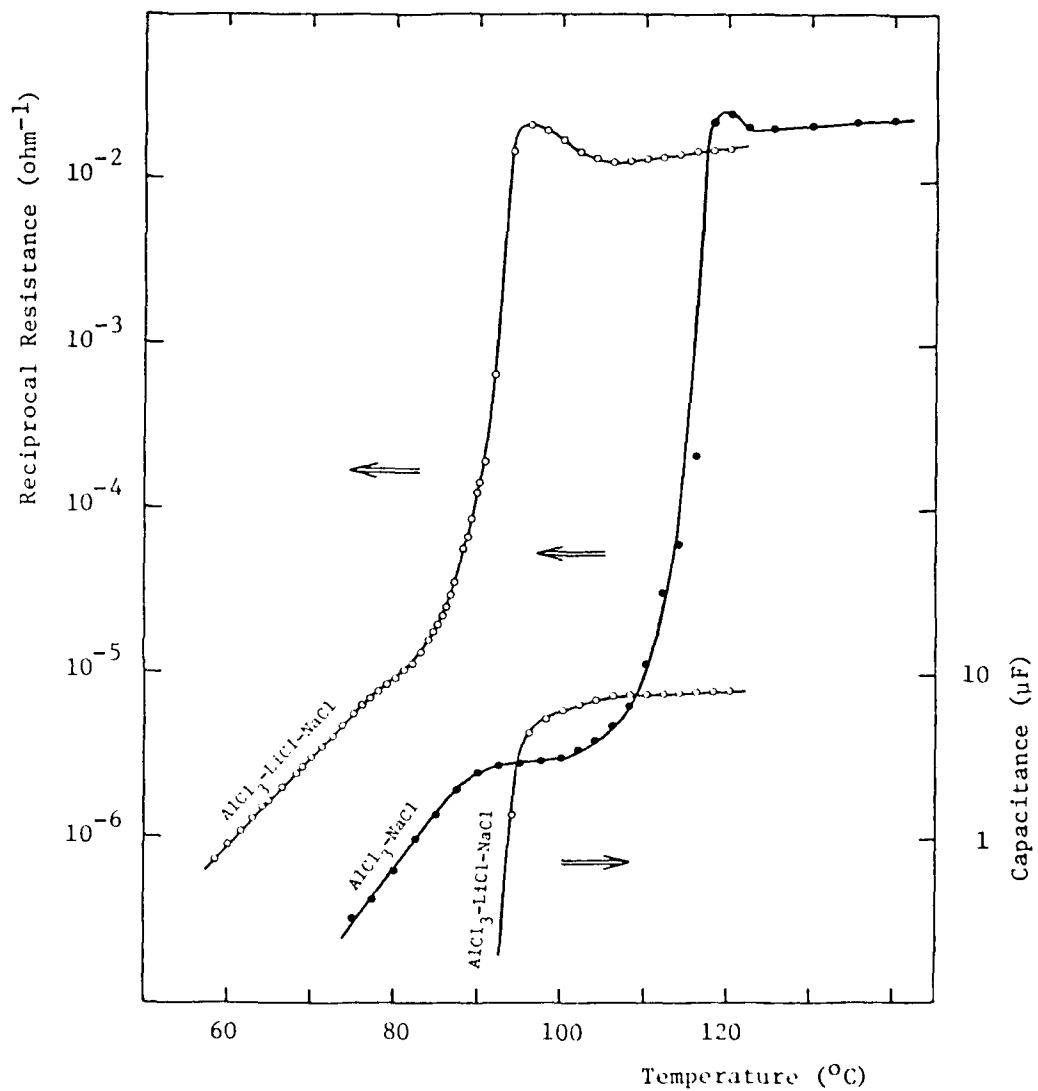


Figure 7. Reciprocal Resistance and Capacitance of 54.0-23.0-23.0 Mole % AlCl_3 - LiCl - NaCl and of 66.0-34.0 Mole % AlCl_3 - NaCl .

REFERENCES

1. For overview of the current status of battery R & D, see Proceedings of the Symposium on Load Levelling, N. P. Yao and J. R. Selman, eds., The Electrochemical Society, Princeton, N.J., 1977.
2. D. M. Ryan and L. C. Bricker, Report AFAPL-TR-77-12, April 1977.
3. G. Mamantov, in Proceedings of NATO Institute on Advanced Batteries, in press.
4. G. J. Janz, C. B. Allen, N. P. Bansal, R. M. Murphy and R. P. T. Tomkins, Report NSRDS-NBS61, Part 2, April 1979.
5. G. Mamantov and R. A. Osteryoung in Characterization of Solutes in Non-aqueous Solvents, G. Mamantov, ed., Plenum Press, N.Y. 1978.
6. H. L. Chum, V. R. Koch, L. L. Miller and R. A. Osteryoung, J. Amer. Chem. Soc., 97, 3264 (1975).
7. V. R. Koch, L. L. Miller and R. A. Osteryoung, J. Amer. Chem. Soc., 98, 5277 (1976).
8. C. L. Hussey, J. C. Nardi, L. A. King, and J. K. Erbacher, J. Electrochem. Soc., 124, 1451 (1977); C. L. Hussey, private communication.
9. R. A. Carpio, L. A. King, R. E. Lindstrom, J. C. Nardi and C. L. Hussey, J. Electrochem. Soc., 126, 1644 (1979).
10. G. J. Janz, C. B. Allen, J. R. Downey, Jr., and R. P. T. Tomkins, ERDA Report TID 27163-P1 and P2, July 1976.
11. P. V. Clark, Report SC-R-68-1680, vols. 1 and 2, 1968.
12. J. Kendall, E. D. Crittenden and H. K. Miller, J. Amer. Chem. Soc., 45, 976 (1923).
13. E. M. Levin, J. F. Kinney; R. D. Wells and J. T. Benedict, J. Res. Nat. Bur. Stand., 78A, 505 (1974).
14. W. P. Brennan, B. Miller, and J. C. Whitwell, Proc. 2nd Symp. Analytical Calorimetry, R. S. Porter, ed., Plenum Press, New York, 1970.
15. J. L. McNaughton and C. T. Mortimer, in IRS, Physical Chemistry, Series 2, Vol. 10, Butterworths, London, 1975, reprinted by the Perkin Elmer Co.
16. E. Pella and M. Nebuloni, J. Thermal Anal., 3, 229 (1971).
17. R. A. Carpio, personal communication.
18. R. Midorikawa, J. Electrochem. Soc. Japan, 23, 72, 127 (1955).

19. M. D. Pyatunin, A. V. Storonkin and I. V. Vasil'kova, Vestnik Leningrad. Univ., Ser. Fiz. Khim., 165 (1973).
20. M. A. Kuvakin, L. I. Talanova and A. I. Kulikova, Russ. J. Inorg. Chem., 18, 602 (1973).
21. C. T. H. M. Cronenberg and J. W. Van Spronsen, Z. Anorg. Allg. Chem., 354, 103 (1967).
22. V. I. Mikheeva, S. M. Arkhipov and T. V. Revzina, Russ. J. Inorg. Chem., 13, 884 (1968).
23. E. Ya. Gorenbein, Zhur. Obshch. Khim., 18, 1427 (1948); 19, 1978 (1949).
24. J. A. Plambeck, J. Chem. Eng. Data, 12, 77 (1967).
25. G. Jones and B. C. Bradshaw, J. Amer. Chem. Soc., 55, 1790 (1933).
26. R. A. Robinson and R. H. Stokes, Electrolyte Solutions, 2nd ed., Butterworths, London 1970.